Crack Growth in Noncrystalline Solids

Maximilien E. Launey[1], Robert O. Ritchie[1,2]
[1]Department of Materials Science and Engineering, University of California, Berkeley, CA, USA
[2]Lawrence Berkeley National Laboratory, Berkeley, CA, USA

Synonyms

Bulk metallic glass (BMG); Fatigue transformation zone (FTZ); Glass-forming ability (GFA); Glass-transition temperature (T_g); Long-range order (LRO); Medium-range order (MRO); Shear transformation zone (STZ); Short-range order (SRO)

Definition

Crack growth in amorphous metals pertains to the extension of incipient cracks or flaws in metals that exhibit a glass transition and no long-range order (LRO) – or periodicity – characteristic of a crystal.

Scientific Fundamentals

Atomic Structure of Metallic Glasses

The glassy state is reached when a cooled liquid solidifies without crystallization, which is associated with the phenomena of the glass transition. No pure metals and few metallic alloys are natural glass-formers. The first reported amorphous alloy with a composition of $Au_{75}Si_{25}$ was produced by the rapid cooling of a metallic liquid (Klement et al. 1960). In the early days of research on metallic glasses, high cooling rates of the order of 10^5–10^6 K/s were usually required for glass formation from most alloys, thereby restricting the resulting material to thin ribbons, foils, and powders, where at least one dimension was small enough (~ micrometers) to permit such a high cooling rate. A major challenge, therefore, has been to obtain glassy alloys in bulk form in a simple operation such as casting. The critical size of bulk metallic glasses (BMGs) is defined as the maximum possible value of the minimum dimension (such as the diameter of a rod) that permits the sample to be fully glassy. Despite encouraging results on noble-metal–based compositions in the early 1980s, it took until the 1990s for most BMG-forming compositions to be discovered (Peker and Johnson 1993; Inoue 2000).

Systematic research since then has identified the key thermodynamic and kinetic factors that lead to alloy compositions with particularly good glass-forming ability (GFA). In essence, the alloy melt should have (1) a low entropy and enthalpy and therefore a low thermodynamic driving force for crystallization, and (2) low atomic mobility associated with a viscosity that is high and comparatively weakly temperature-dependent, kinetically suppressing the crystallization. These factors are linked, having their origin in a densely packed liquid structure with pronounced short- and medium-range order (SRO and MRO, respectively).

It is well known that the mechanical properties of crystalline materials are strongly reliant on their crystal and electronic structures. This intrinsic relationship has been well established with the development of dislocation theory and electronic theory, which can explain, in general, the atomic and electronic origins of the strength and ductility of crystalline materials. In contrast, for disordered materials, such as metallic glasses, a definite correlation between their mechanical behavior and atomic and electronic structures has yet to be properly established. Basic knowledge of the controlling factors of the strength and ductility of metallic glasses at temperatures well below their glass-transition temperatures (T_g) is actually poor. BMGs exhibit no long-range order (LRO) as they are solidified from liquid without reaching the crystalline ground state; however, SRO and MRO structural order does develop to a considerable extent, under the given kinetic constraints, as the atoms strive to find comfortable configurations to lower their energy. SRO develops over the first couple of coordination shells (typically <0.5 nm), beyond which medium-range order (MRO) may extend to beyond ~1 nm. SRO and MRO are inherent local structures in the glassy state, not just quenched-in crystallizing phases that are not fully suppressed during solidification. For a monolithic glass, it is the short- and medium-range order that is expected to control its mechanical properties, such as the initiation of plastic flow, given the absence of dislocations with defined Burgers vectors.

Free Volume and Deformation

Strength and ductility, two properties that underlie crack growth behavior in materials, are controlled by the ease and extent of plastic flow, which in metallic glasses occurs via a diffusional process involving the stress-induced cooperative rearrangement of small groups of atoms referred to as *flow defects* or *shear transformation zones* (Spaepen 1977; Argon 1979). These flow defects are associated with atomic scale open spaces, or *free volume* sites, which are distributed throughout the structure. Thus, it is usually assumed that in glasses the amount of free volume controls plastic flow. At high stresses and low temperatures (<0.7 T_g), plastic deformation is inhomogeneous

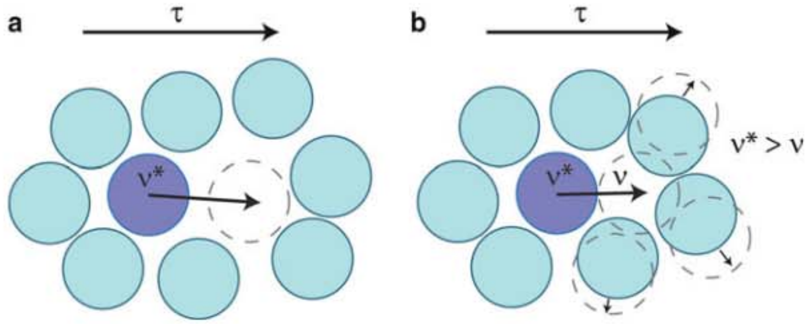

Crack Growth in Noncrystalline Solids, Fig. 1 Illustration of (**a**) an individual atomic jump – the basic step for macroscopic diffusion and flow, and (**b**) creation of free volume by squeezing an atom of volume v^* into a neighboring hole of smaller volume (Reproduced from Spaepen (1977))

(i.e., flow is highly localized in thin shear bands); in contrast, at high temperatures the plastic flow is homogeneous at low stresses and each volume undergoes the same strain.

The microscopic mechanism that governs both homogeneous and inhomogeneous flow has been described by (Spaepen 1977) and is illustrated in Fig. 1. It is assumed that macroscopic flow occurs as a result of a number of individual atomic jumps. In order for a jump to occur, it must have a nearest neighbor environment (Fig. 1a), that is, next to it there must be a hole large enough to accommodate its appropriate hard-sphere equivalent atomic volume v^*. In order to make the jump, some activation energy must be supplied. If no external force is present, this is obtained from thermal fluctuations; the number of jumps across the activation barrier is the same in both directions. This is the basic microscopic mechanism for diffusion. When an external force (e.g., a shear stress) is applied, the atomic jumps occurs in the direction of the force; the number of forward jumps across the activation barrier is larger than the number of backwards jumps, which results in a net forward flux of atoms and forms the basic mechanism for flow. If the applied shear stress is large enough, free volume could be created as an atom with volume v^* squeezes into a neighboring free volume site with slightly smaller volume v, increasing the free volume by $v^* - v$ (Fig. 1b). Competing with this creation process is a relaxation process in which subtle rearrangements annihilate free volume. At low stresses, the annihilation rate exactly balances the creation rate and the free volume remains constant. However, at high stresses, the creation rate exceeds the annihilation rate, resulting in catastrophic softening as the free volume increases dramatically. As the stress drops, the driving force for free volume creation declines until a new, larger steady state free volume is established. However, if a band of material is perturbed to a slightly higher initial free volume than its surroundings, the catastrophic softening event is associated with strain localization in the band. Thus, after the localization event, the free volume within the shear band should be measurably greater than in the undeformed material, increasing the average free volume overall.

After inhomogeneous deformation, metallic glass failure surfaces exhibit characteristic vein and void patterns (Fig. 3) indicative of significant softening on the failure plane. Thus, flow models that lead to strong softening in shear bands have been proposed. The concept of shear transformation zone (STZ) was introduced (Argon 1979) to explain the plastic deformation of metallic glasses (Fig. 2). Generally, thermally activated STZs initiate around free volume sites under an applied shear stress because high elastic strain at free volume sites energetically promotes STZs formation. The ability of a region to undergo a shear transformation depends on the local atomic density (i.e., the amount of free volume). The free volume is assumed to be distributed statistically among all the atoms in the material. This implies that there is a similar statistical distribution of flow defects with sufficient free volume to enable shear transformation at a given stress.

Mechanisms of Fatigue-Crack Growth

In the fully amorphous metals, stable fatigue-crack growth is readily observed under cyclic loading (Gilbert et al. 1999). Such growth rate behavior, da/dN, is plotted in Fig. 4 as a function of the stress-intensity range, ΔK, for a $Zr_{41.2}Ti_{13.8}Cu_{12.5}Ni_{10}Be_{22.5}$ (commercially known as Vitreloy1™) BMG specimen tested at a load ratio (ratio of minimum to maximum load, $R = P_{min}/P_{max}$) of 0.1 and

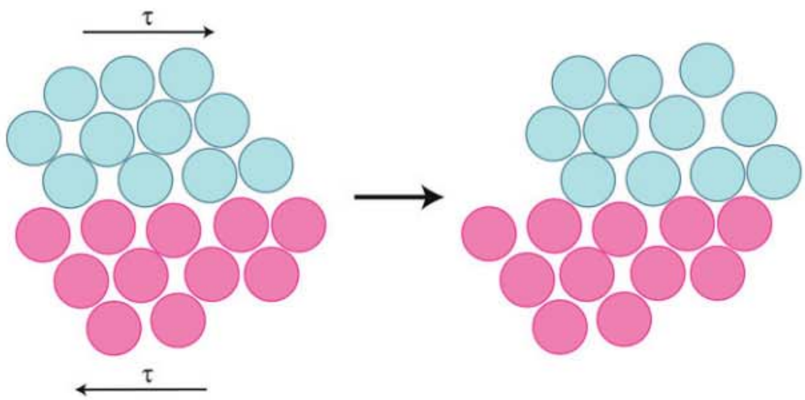

Crack Growth in Noncrystalline Solids, Fig. 2 A shear displacement occurs to accommodate an applied shear stress τ (Reproduced from Argon (1979))

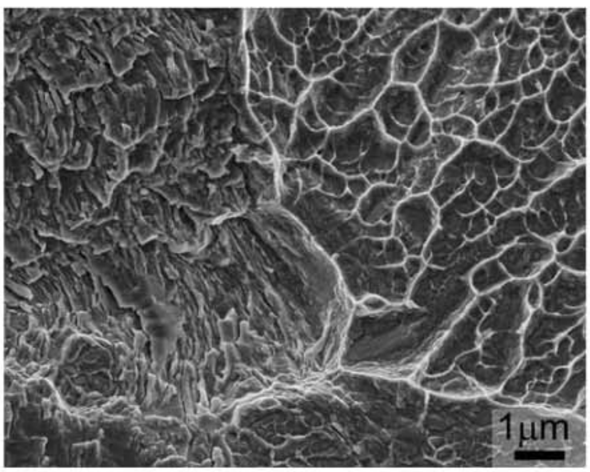

Crack Growth in Noncrystalline Solids, Fig. 3 SEM image of a fracture surface of a $Zr_{44}Ti_{11}Cu_{10}Ni_{10}Be_{25}$ monolithic BMG after fatigue-crack growth test showing the transition between stable growth and unstable fracture. Fatigue striations are typically observed in the stable growth regime, while a vein-like morphology is typical of overload fracture in amorphous metals. The nominal crack growth direction is here from *left* to *right*

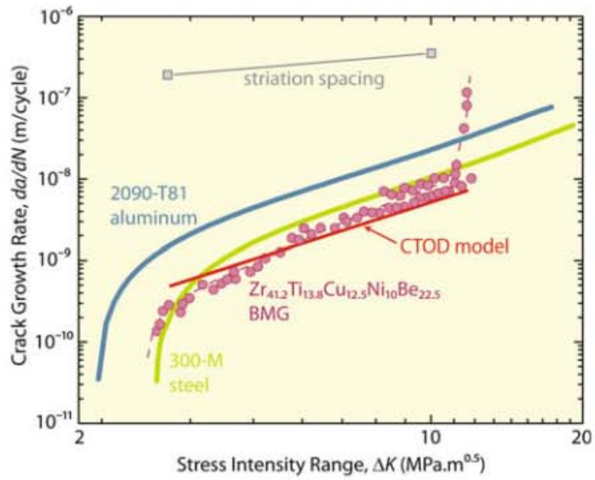

Crack Growth in Noncrystalline Solids, Fig. 4 Fatigue-crack propagation for a $Zr_{41.2}Ti_{13.8}Cu_{12.5}Ni_{10}Be_{22.5}$ monolithic BMG scaled with the $\Delta CTOD = 0{:}01\ \Delta K^2/\sigma_Y E'$ (where σ_Y is the flow stress and E' is the appropriate Young's modulus) and corresponding striation spacings. Also shown for comparison are growth-rate results for polycrystalline metals, namely 300-M high-strength steel and 2090-T81 aluminum–lithium alloy (Reproduced from Gilbert et al. (1999))

a frequency of 25 Hz. Behavior is compared with that of an ultrahigh-strength steel (300-M) and an age-hardened aluminum alloy (2090-T81); indeed, in general, cyclic crack growth rates in amorphous metals are comparable to those observed in traditional polycrystalline metallic alloys. This can be seen by regression fitting these data to the basic Paris power-law relationship:

$$\frac{da}{dN} = C'\Delta K^m, \tag{1}$$

where m is the crack-growth exponent and C' is a scaling constant. It can be seen that the exponent m in the mid-range of growth rates ($\sim 10^{-10}$ to 10^{-7} m/cycle) lies in the range of $m \sim 2$–5 (Fig. 4), typical of ductile crystalline metals in this regime. These values of m are in marked contrast to the fatigue properties of ceramics and oxide glasses, where m typically lies in the range of $m \sim 15$–50. Values of the fatigue threshold, ΔK_{TH}, in the metallic glass ranged from ~ 1 to 3 MPa$\sqrt{m}$, again comparable to many high-strength steel and aluminum alloys.

Fatigue striations are observed on the fatigue surfaces at both low and high driving forces (Fig. 3). Although not uniformly covering the fracture surface, the striation spacing scales with growth rates, as plotted in Fig. 4. Moreover, consistent with measurements in rapidly quenched metallic glasses ribbons, the striation spacings significantly overestimate the macroscopic growth rates. This effect is typical of metallic materials at growth rates below 10^{-6} m/cycle and is associated with the non-uniform crack extension along the crack front. The mechanism of striation formation in crystalline is associated with irreversible crack-tip shear that alternately blunts and resharpens the crack during the fatigue cycle. Models for striation formation indicate that growth rates should scale with the range of crack-tip opening displacement ($\Delta CTOD$). Using simple continuum-mechanics arguments,

$$\frac{da}{dN} \propto \Delta CTOD \approx \beta' \frac{\Delta K^2}{\sigma_Y E'}, \qquad (2)$$

where σ_Y is the flow stress, $E' = E$ (Young's modulus) in plane stress or $E/(1-\nu^2)$ in plane strain, and β' is a scaling constant ($\sim$0.01–0.1 for mode I crack growth), which is a function of the degree of slip reversibility and elastic–plastic properties of the material. As slip (shear) bands form readily in amorphous metals, Eq. (2) provides a reasonable description of the experimentally measured growth rates with $\beta' \sim 0.01$ (Fig. 4). Together with the presence of fatigue striations on the fracture surfaces, this suggests a mechanism for cyclic crack advance in metallic glasses, which also involves repetitive blunting and resharpening of the crack tip.

Role of free volume: It is now well accepted that a reduction in free volume by structural relaxation embrittles bulk metallic glasses. Existing models for the deformation of metallic glasses predict that a reduction in free volume will inhibit plastic deformation (Spaepen 1977; Argon 1979), and it logically follows that the reduced ductility results in less crack-tip blunting and lower fracture toughness (Gilbert et al. 1999; Launey et al. 2008). It is perhaps surprising that fatigue-crack growth, which is believed to result from alternating crack blunting and resharpening, is not affected by change in the free volume (Launey et al. 2008). During inhomogeneous plastic flow in BMGs, the deformation is highly localized in shear bands and it has been reasoned that the observed softening in those shear bands must be due to local free volume generation within the bands (Spaepen 1977; Argon 1979). Experimental studies (Flores et al. 2002) have given direct evidence of free volume increases associated with plastic flow during compression in bulk metallic glasses using positron annihilation spectroscopy (PAS). Additionally, molecular-dynamics simulations of binary metallic glass structures and deformation (Shi and Falk 2005) show softening and shear localization that is associated with free volume production. Thus, based on the current understanding of flow in metallic glasses, it is expected that the large plastic strains near a crack tip will be associated with a local increase in free volume. It has been proposed that this deformation-induced free volume determines the local flow properties, rendering fatigue-crack growth behavior relatively insensitive to initial bulk free volume differences (Launey et al. 2008). PAS provides an experimental capability to examine subatomic open volumes and is therefore useful for directly analyzing the free volume in amorphous materials. Indeed, it has been used to demonstrate the presence of a *fatigue transformation zone* (FTZ) of enhanced free volume that is generated by a propagating fatigue crack tip (Liu et al. 2009). Those results have suggested that (1) fatigue cycling induces a FTZ ahead of the crack tip that has distinctly larger free volume voids than the bulk, and (2) the thickness of the FTZ is roughly similar to the expected cyclic plastic zone that is roughly a quarter of the total plastic zone size:

$$r_{FTZ} = \frac{1}{8\pi}\left(\frac{K_{max}}{\sigma_Y}\right)^2, \qquad (3)$$

where K_{max} and σ_Y are the maximum stress intensity and yield strength, respectively. The transformation zone discussed is similar to the martensitic transformation zones that occur in partially stabilized zirconia or austenitic stainless steel, although in those cases the volume increase is due to a phase transformation from one crystal structure to another. In those cases, the large volume expansion (2–4%) associated with the martensitic transformation generates a residual stress field that puts the crack under compression, reducing crack propagation rates. In BMGs, the total volume increase is orders of magnitude smaller and is not large enough to cause significant compressive stresses on the crack tip based on models for transformation toughening (Evans and Cannon 1986). Using the weight function method developed by McMeeking and Evans (1982), a 1 MPa$\sqrt{m}$ reduction in the maximum stress intensity at the crack tip near the threshold would require a total volume expansion of $\sim$10% within a 100 nm thick transformation zone. Additionally, the average free volume per atom of the $Zr_{44}Ti_{11}Ni_{10}Cu_{10}Be_{25}$ bulk metallic glass was found to

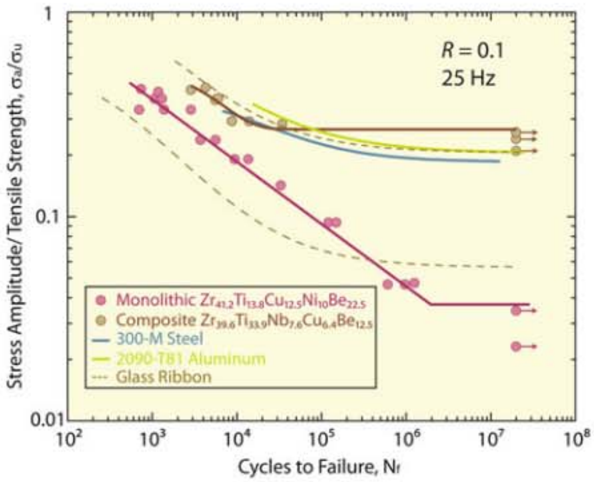

Crack Growth in Noncrystalline Solids, Fig. 5 *S-N* curve for a $Zr_{41.2}Ti_{13.8}Cu_{12.5}Ni_{10}Be_{22.5}$ monolithic BMG and a $Zr_{39.6}Ti_{33.9}Nb_{7.6}Cu_{6.4}Be_{12.5}$ composite BMG. Also shown for comparison are *S-N* curves for polycrystalline metals, namely 300-M high-strength steel and 2090-T81 aluminum–lithium alloy (Reproduced from Launey et al. (2009))

represent roughly ~0.1% of the total volume when considering only the smallest atoms (beryllium) and the hard sphere model (Launey et al. 2008). Therefore, this means that the free volume would have to expand by two orders of magnitude in order to decrease the stress intensity by 1 MPa√m near the fatigue threshold. Thus, the total volume increase by free volume expansion in BMGs is largely insufficient to generate a significant compressive residual stress field.

Mechanisms of Fatigue-Crack Initiation

The stress-life (*S/N*) data in Fig. 5 present an interesting contrast between crystalline and amorphous metals. Whereas the crack-propagation properties (Fig. 4) are similar in the two classes of materials (with respect to the presence of fatigue striations and the dependence of growth rates on ΔK), the stress/life behavior (Fig. 5) is markedly different (Gilbert et al. 1999; Menzel and Dauskardt 2006). In the *S/N* measurements on BMGs, total life is far less dependent upon the applied stress amplitude, and the fatigue limit can be as low as $\sigma_a/\sigma_{UTS} \sim 0.04$, where σ_a is the applied stress amplitude ($\sigma_a = (\sigma_{max} - \sigma_{min})/2$), normalized by the tensile strength, σ_{UTS}. This is one order of magnitude lower than their crystalline counterparts. It implies that mechanistically the fatigue properties of crystalline and amorphous metals differ significantly with respect to crack *initiation*, or, more precisely, in the nucleation of crack growth. Such a difference is thought to be associated with the easier natural initiation of a fatigue crack (e.g., via slip-band formation) in BMGs. Damage evolution occurs very early during fatigue loading with very few, if any, loading cycles associated with damage initiation processes (Menzel and Dauskardt 2006). The fatigue life is therefore dominated by the number of cycles needed to propagate the damage to critical size, unlike high-strength single or polycrystalline metals where the damage initiation step normally represents the majority of high-cycle fatigue life. The lack of a significant damage initiation stage in amorphous metals has been shown to account for their low fatigue or endurance limits. Furthermore, since the fatigue limit can be equated with the critical stress for crack initiation or, more generally, for an initiated (small) crack to overcome some microstructural "barrier" (e.g., a grain boundary), it is presumed that the markedly lower fatigue limits in the amorphous alloys are associated primarily with a lack of microstructure, which would normally provide local arrest barriers to newly initiated or pre-existing cracks. Indeed, in this regard low fatigue limits appear to be a characteristic of monolithic metallic glasses.

Recent studies on the development of bulk metallic-glass matrix composites, however, have found effective means to mitigate this problem by introducing local crack-arresting barriers back into the microstructure (Launey et al. 2009). By introducing a second phase in form of crystalline dendrites, and by creating an effective interaction between the length-scales of the shear bands and that of the dendrites, the fatigue limit can be raised significantly, by as much as an order of magnitude, to approach values comparable to that of high-strength crystalline metallic materials (Fig. 5). As noted above, small cracks are observed to initiate after only a few stress cycles in BMGs (Menzel and Dauskardt 2006). In contrast to crystalline alloys, fatigue lifetimes should therefore be governed by early crack propagation (rather than initiation), specifically by the number of cycles to extend a small flaw to some critical size. In the case of BMG-matrix composites, the formation of single-shear band motivated failures can be prevented by making the critical flaw size for unstable crack growth larger than some feature of the dendritic microstructure (i.e., the interarm spacing). To prevent a shear band from opening and causing failure between dendrite arms, the shear band length must be less than this critical size which is determined by the applied stress and fracture toughness of the BMG. For high-cycle fatigue resistance, the dendrites must also limit microcrack growth (during 10^7 cycles) in the fatigue limit to a similar length. This argument can be illustrated

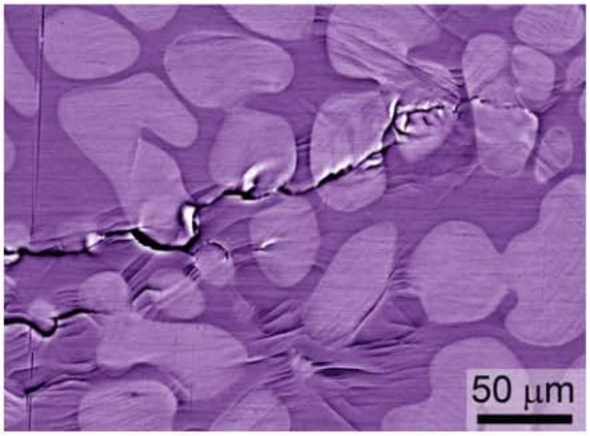

Crack Growth in Noncrystalline Solids, Fig. 6 SEM backscattered electron image of a fatigue crack on the tensile surface showing wide distribution of damage around the crack tip

with a simple fracture-mechanics calculation. If the interdendritic shear bands (see Fig. 6) are modeled as small edge cracks loaded in bending, the approximate stress intensity at the tip of a single interdendritic shear band of 2 μm length would be on the order of 1.9 MPa√m at the stress corresponding to the fatigue limit of $\sigma_a = 0.3\ \sigma_{UTS}$. This is roughly equal to the measured fatigue crack-growth threshold stress intensity for the monolithic glass (Gilbert et al. 1999) and is consistent with no failure in the BMG-composite at 2×10^7 cycles. In contrast, for a glass-matrix composite with a smaller volume fraction of dendrites and interdendritic glass thicknesses of ~10 μm (Flores et al. 2003), a shear band could grow five times larger before arrest by the dendrites. The threshold stress intensity can now be reached at much lower applied stress of $\sigma_a = (0.3/5^{1/2})\sigma_{UTS} \sim 0.1\sigma_{UTS}$, as observed experimentally. This presents a simple hypothesis for improving the low fatigue limits in metallic glasses. The characteristic spacing, D, which separates second-phase inclusions in a glassy matrix (and thereby confines the shear band length) should be such that $\alpha\sigma_a D^{1/2} \sim K_{th}$ where K_{th} is the critical stress-intensity threshold for fatigue-crack propagation in the monolithic glass and α is a constant of order unity. Equivalently, one predicts a fatigue limit of $\sigma_a \sim K_{th}/\alpha D^{1/2}$. In the absence of any microstructure, as in *monolithic* BMG, it is clear that fatigue limits will be very low since D becomes essentially infinitely large.

Role of free volume: Free volume relaxation does not have much influence on fatigue crack-growth rates, da/dN, and fatigue thresholds, ΔK_{th}. However, a reduction of free volume can improve the fatigue limit, thereby increasing fatigue lifetimes (Launey et al. 2008). It was shown that these effects are associated primarily with the crack initiation stage of the fatigue lifetime. Mechanistically, this may be understood by considering that fatigue cracks tend to initiate from slip bands. A larger amount of free volume in the material allows easier deformation and easier formation of slip bands, leading to faster crack initiation, possibly caused by nanovoids or nanocrystals that form within the shear bands that act as damage initiation sites. For example, in the absence of residual stresses, a monolithic $Zr_{44}Ti_{11}Ni_{10}Cu_{10}Be_{25}$ BMG was found to spend most of its fatigue life in crack initiation (Launey et al. 2008); this is in sharp contrast with results on the same alloy composition that reported that fatigue crack initiation occurs within the first few cycles (Menzel and Dauskardt 2006). It is currently unclear why these materials behaved so differently, but possibilities include (1) fundamental differences between the alloys, and/or (2) other factors such as residual stresses, defects, or other inhomogeneities. With respect to the latter, the test specimens in the Menzel and Dauskardt (2006) study were not stress relieved, and depending on the orientation and machining of the beams, residual tensile stresses on the tensile surface during the bending tests may have contributed to premature crack initiation. Additionally, defects or inhomogeneities in the BMG could also have accounted for much quicker crack initiation.

Effects of Residual Stresses

Bulk metallic glasses develop residual stresses during processing due to thermal tempering. It has been shown that compressive stresses on the order of several hundred MPa can occur on the surface of as-cast metallic glasses, with offsetting tensile stresses below the surface. The effects of residual stresses have often been ignored in the published literature on mechanical properties of BMGs; however, residual compressive stresses on the specimen surfaces can reduce the crack-propagation rate in the threshold region and improve the fracture toughness. A study on monolithic BMG showed that these increases were significant, 33% and 50% increases for ΔK_{TH} and K_{IC}, respectively (Launey et al. 2008). Furthermore, although not explicitly measured in this study, those combined effects are expected to have a significant effect on the overall fatigue lifetime. The mechanism responsible for these effects is presumed to be that the compressive thermal tempering stresses superimpose onto the crack-tip stress field, and thereby lower the stress intensity at the crack tip. Although that mechanism only acts on the specimen surfaces where the residual stresses are compressive, it is clearly significant enough to affect the overall properties. The effect of residual stresses likely explains some of the scatter observed in published fracture and fatigue data, such as the large scatter in ΔK_{TH} seen in (Gilbert et al. 1999). Thus, when testing BMGs without first relieving the residual stresses, it is important that the residual stresses be characterized and reported along with the data.

Key Applications

Amorphous metals (metallic glasses) offer attractive benefits, combining some of the desirable properties of conventional crystalline metals and the formability of conventional oxide glasses. For example, in the absence of the well-defined dislocation defects ubiquitous in crystalline alloys, metallic glasses exhibit room-temperature strength much closer to the theoretical strength of the material than their crystalline counterparts. Meanwhile, near-net-shape processing can be realized by exploiting the viscous flow in the supercooled-liquid regime. Cast glassy alloys exhibit a shiny finish and maintain dimensional accuracy, avoiding shrinkage associated with crystallization. The absence of grain boundaries in glassy alloys contributes to unique combinations of magnetic, electrical, chemical, and tribological properties.

Cross-References

- ▶ Crack Growth in Brittle and Ductile Solids
- ▶ Crack Initiation in Brittle Solids
- ▶ Cyclic Loading and Cyclic Stress
- ▶ Damage Accumulation
- ▶ Fatigue
- ▶ Fatigue Limit
- ▶ Stress Intensity Factors
- ▶ Stress-Life Theories

References

A.S. Argon, Plastic-deformation in metallic glasses. Acta Metall. **27**(1), 47–58 (1979)

A.G. Evans, R.M. Cannon, Toughening of brittle solids by martensitic transformations. Acta Metall. **34**(5), 761–800 (1986)

K.M. Flores et al., Characterization of free volume in a bulk metallic glass using positron annihilation spectroscopy. J. Mater. Res. **17**(5), 1153–1161 (2002)

K.M. Flores et al., Fracture and fatigue behavior of a Zr-Ti-Nb ductile phase reinforced bulk metallic glass matrix composite. Scr. Mater. **49**(12), 1181–1187 (2003)

C.J. Gilbert et al., Mechanisms for fracture and fatigue-crack propagation in a bulk metallic glass. Metall. Mater Trans.-Phys. Metall. Mater. Sci. **30**(7), 1739–1753 (1999)

A. Inoue, Stabilization of metallic supercooled liquid and bulk amorphous alloys. Acta Mater. **48**(1), 279–306 (2000)

W. Klement et al., Non-crystalline structure in solidified gold-silicon alloys. Nature **187**(4740), 869–870 (1960)

M.E. Launey et al., Effects of free volume changes and residual stresses on the fatigue and fracture behavior of a Zr-Ti-Ni-Cu-Be bulk metallic glass. Acta Mater. **56**(3), 500–510 (2008)

M.E. Launey et al., On a solution to the problem of the poor cyclic fatigue resistance of bulk metallic glasses. Proc. Natl. Acad. Sci. U.S.A. **106**(13), 4986–4991 (2009)

M. Liu et al., Assessment of the fatigue transformation zone in bulk metallic glasses using positron annihilation spectroscopy. J. Appl. Phys. **105**, 093501 (2009)

R.M. McMeeking, A.G. Evans, Mechanics of transformation-toughening in brittle materials. J. Am. Ceram. Soc. **65**(5), 242–246 (1982)

B.C. Menzel, R.H. Dauskardt, Stress-life fatigue behavior of a Zr-based bulk metallic glass. Acta Mater. **54**(4), 935–943 (2006)

A. Peker, W.L. Johnson, A highly processable metallic-glass: $Zr_{41.2}Ti_{13.8}Cu_{12.5}Ni_{10.0}Be_{22.5}$. Appl. Phys. Lett. **63**(17), 2342–2344 (1993)

Y.F. Shi, M.L. Falk, Strain localization and percolation of stable structure in amorphous solids. Phys. Rev. Lett. **95**(9), 095502 (2005)

F. Spaepen, Microscopic mechanism for steady-state inhomogeneous flow in metallic glasses. Acta Metall. **25**(4), 407–415 (1977)

Crack Initiation in Brittle Solids

Kan Ding
Swinburne University of Technology, Hawthorn, Victoria, Australia

Synonyms

Fracture initiation in brittle solids

Definition

Crack initiation is due to a solid body subjected to cyclic or fatigue loads, which experience localized stresses in the vicinity of the concentration feature, which exceed the conventional strength or failure limit of the material.

Scientific Fundamentals

Fracture Mechanics Approach

Fracture mechanics is an important tool for understanding the formation of cracks in materials. The theory was first developed by Griffith (1920), who found the fracture energy relationship during his experiments on glass fibers. The experimental results indicated that the product of the square root of the flaw length (l) and the stress at fracture (σ_f) was nearly constant C, which is expressed by the equations

$$\sigma_f\sqrt{l} \approx C \qquad (1)$$

$$C = \sqrt{\frac{2E\gamma}{\pi}} \qquad (2)$$